nature communications

Article

https://doi.org/10.1038/s41467-024-50921-w

Sequence-specific nanoparticle barcode strategy for multiplex human enterovirus typing

Received: 2 November 2023

Accepted: 23 July 2024

Published online: 01 August 2024

Check for updates

Zecheng Zhong[1,2,3,8], Xiaosong Su[4,8], Kunyu Yang[1,2,3,8], Weida Huang[1,2,3], Jin Wang[1,2,3], Zhihao Zhuo[1,2,3], Jiyu Xiang[1,2,3], Lesi Lin[1,2,3,5], Shuizhen He[6], Tingdong Li[1,2,3,7], Jun Zhang[1,2,3,7], Shengxiang Ge[1,2,3,7] ✉, Shiyin Zhang[1,2,3,7] ✉ & Ningshao Xia[1,2,3,5,7] ✉

Human enteroviruses (HEV) can cause a range of diseases from mild to potentially life-threatening. Identification and genotyping of HEV are crucial for disease management. Existing typing methods, however, have inherent limitations. Developing alternative methods to detect HEV with more virus types, high accuracy, and sensitivity in an accessible manner presents a technological and analytical challenge. Here, a sequence-specific nanoparticle barcode (SSNB) method is presented for simultaneous detection of 10 HEV types. This method significantly increases sensitivity, enhancing detection by 10-10^6 times over the traditional multiplex hybrid genotyping (MHG) method, by resolving cross-interference between the multiple primer sets. Furthermore, the SSNB method demonstrates a 100% specificity in accurately distinguishing between 10 different HEV types and other prevalent clinical viruses. In an analysis of 70 clinical throat swab samples, the SSNB method shows slightly higher detection rate for positive samples (50%) compared to the RT-PCR method (48.6%). Additionally, further assessment of the typing accuracy for samples identified as positive by SSNB using sequencing method reveals a concordance rate of 100%. The combined high sensitivity and specificity level of the methodology, together with the capability for multiple type analysis and compatibility with clinical workflow, make this approach a promising tool for clinical settings.

The enterovirus genus is one of the most common in the family Picornaviridae and includes four HEV species (EV-A, B, C, and D)[1]. More than 300 different enterovirus serotypes have been identified[2], that cause a variety of diseases, including respiratory, skin, neurologic, and gastrointestinal[3]. Each year, there are over one billion estimated new enterovirus infections; some of these, such as EV71 and CVA16, have been responsible for multiple outbreaks of hand, foot, and mouth disease (HFMD) in Asia and Europe[4–6], while an EV-D68 epidemic has

[1]State Key Laboratory of Vaccines for Infectious Diseases, School of Public Health, Xiamen University, Xiamen 361102 Fujian, China. [2]NMPA Key Laboratory for Research and Evaluation of Infectious Disease Diagnostic Technology, School of Public Health, Xiamen University, Xiamen 361102 Fujian, China. [3]Xiang An Biomedicine Laboratory, School of Public Health, Xiamen University, Xiamen 361102 Fujian, China. [4]Zhongshan Hospital Fudan University Xiamen Branch, Xiamen 361015 Fujian, China. [5]School of Life Sciences, Xiamen University, Xiamen 361102 Fujian, China. [6]Xiamen Haicang Hospital, Haiyu Road, Xiamen 361026 Fujian, China. [7]State Key Laboratory of Molecular Vaccinology and Molecular Diagnostics, National Institute of Diagnostics and Vaccine Development in Infectious Diseases, National Innovation Platform for Industry-Education Integration in Vaccine Research, Xiamen University, Xiamen 361102 Fujian, China. [8]These authors contributed equally: Zecheng Zhong, Xiaosong Su, Kunyu Yang. ✉e-mail: sxge@xmu.edu.cn; zhangshiyin@xmu.edu.cn; nsxia@xmu.edu.cn

been associated with severe respiratory disease, occasionally leading to acute flaccid myelitis, in Northern America and Europe[7–9]. The widespread prevalence of HEV and their ability to cause severe infections urgently necessitate monitoring and characterization of the HEV types associated with these similar or different clinical manifestations.

Various technologies have been developed for HEV genotyping; however, these have limitations. Virus-neutralization assay[10,11] is time-consuming, labor-intensive, and unable to identify and characterize some of the novel clinical isolates of HEV. RT-PCR offers a rapid and sensitive detection method for HEV, which have been reported to be capable of detecting multiple HEV types[12,13] and higher-throughput HEV detection. However, this method is inherently limited as with an increasing number of primers in the multiplex reaction, the chance of primer dimer formation rises, which subsequently influences detection sensitivity. Furthermore, a small number of PCR fluorescence channels is not suitable for multi-type detection method development. Although nucleic acid hybridization is able to achieve detection of a higher number of targets based on the characteristics of a highly specific gene sequence among different HEV types[14,15], the sensitivity and specificity of this method are poorer than that of RT-PCR. Sequencing part of the *VP1* capsid protein gene is the gold standard for HEV typing[16]; this technique is, however, relatively expensive with long turn-around times, requires a dedicated bioinformatics facility and personnel with high-level expertise, which is not generally available in clinical settings for HEV detection. Thus, the development of multiplex methods, with high accuracy and high sensitivity for HEV genotyping is still challenging.

Here, we show a SSNB platform that capable of detecting and typing 10 HEV in a single tube with high sensitivity. This HEV genotyping platform comprises a barcode that is encoded by sequence-specific nanoparticles, and involves particle phase surface amplification and amplicon-mediated dual-labeled probe decoding for achieving multiplex, in situ HEV genotyping (Fig. 1). Unlike conventional free state primers in liquid phase amplification, type-specific primers are conjugated covalently to distinct nanoparticles. These spatially fixed primers greatly reduced the possible of primer-dimer formation due to free-state primer interaction, thus giving SSNB multiple amplification ability while maintaining exceptionally high sensitivity. Because of the sequence-specific nature of DNA-templated reactions, the covalently linked primers bind to the capture strand and trigger subsequent amplification reactions only in the presence of a perfectly matched target. On the one hand, the nanoparticles marked with dual-labeled probe only in the presence of amplicon on their surface. Because of dually sequence-specific DNA binding reactions, SSNB shows excellent

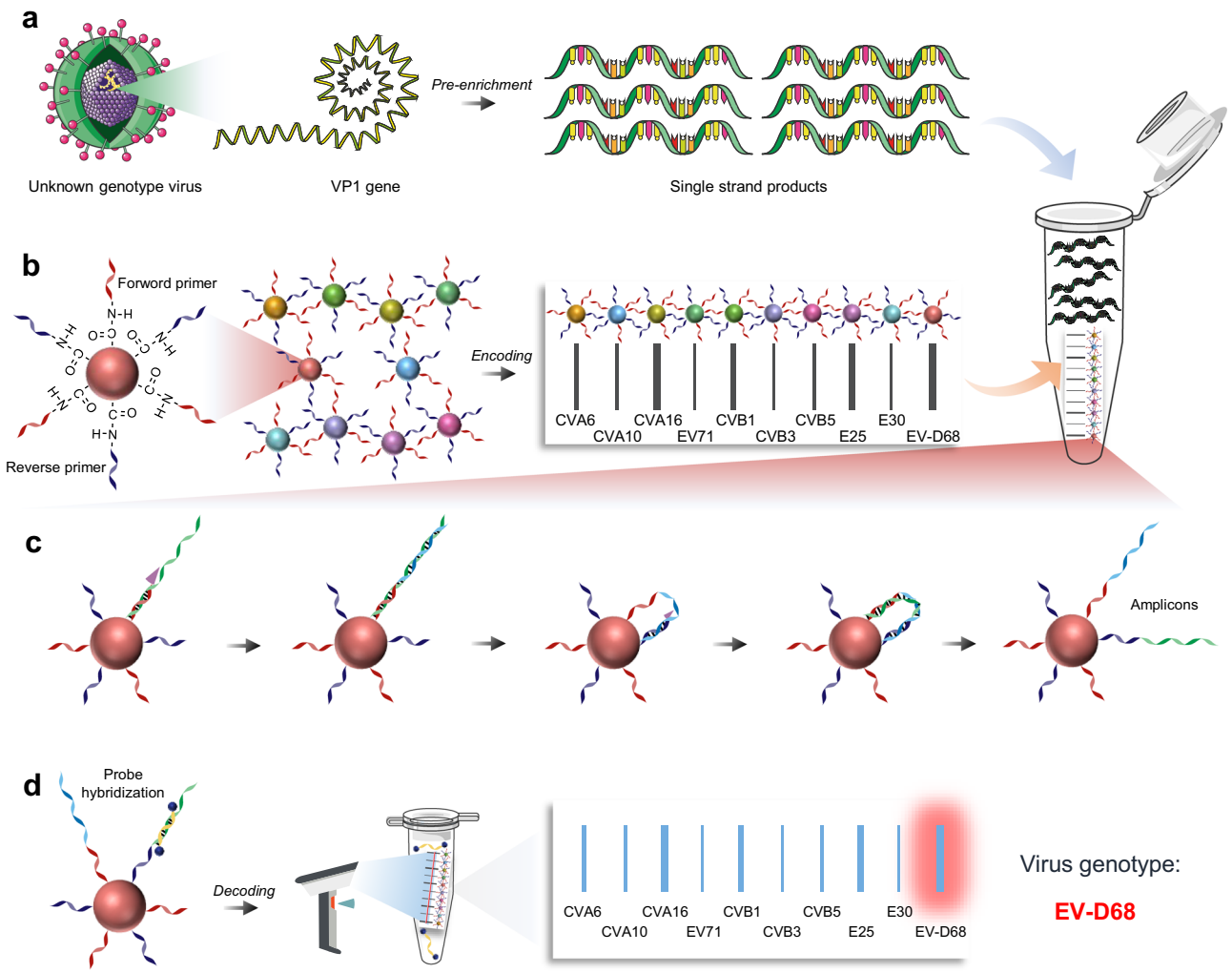

Fig. 1 | Schematic overview of SSNB for HEV genotyping. a The *VP1* gene of HEV was selected and pre-enriched to serve as template. **b** Schematic illustration of the encoding process: type-specific primers coated on different nanoparticles, and mixed together to form a component of the barcode. **c** The particle phase surface amplification process: enriched *VP1* gene products hybridize with specific barcode, and then the particle phase surface amplification is performed on the surface of nanoparticles. **d** Schematic illustration of the decoding process: The probes are hybridized with the amplification products, and the barcode is identified and decoded through two types of fluorescence.

specificity. The nanoparticles we use have unique fluorescence properties, the fluorescence signal of the nanoparticles itself and that on their surface can be identified by a commonly used clinimetric instrument produced by Luminex, and up to 500 nanoparticles[17] paired with an instrument at a time allow accurate recognition, theoretically enabling the genotyping of 500 different HEV types. The SSNB platform offers the advantages of sensitivity, specificity, multiplex ability, and compatibility with clinical routine instruments advantages, which provide the basis for rational decisions in the diagnosis and treatment of HEV and monitoring of infected populations at a regional level; it is therefore of great significance in epidemic control and epidemiological investigation.

Results

Design of SSNB platform

A schematic mechanism for the SSNB platform is shown in Fig. 1. The *VP1* gene of HEV was selected to design primer pairs, the enriched *VP1* gene products were serve as template (Fig. 1a). The encoding process requires a pair of type-specific primers and a fluorescent nanoparticle for HEV genotyping of each target gene. We designed the primers for each type of HEV to capture the *VP1* gene sequence, each of which is incorporated into a distinct nanoparticle, with multiple primers immobilized in a compartmentalized manner within particles. Different types of primer-labeled nanoparticles were mixed and defined as the barcode (Fig. 1b). The barcode was put into a single reaction tube that contained the enriched *VP1* gene products, and the products were recognized by the coding nanoparticles, particle phase surface amplification start from primer extension reaction. The extension products hybridize with immobilized reverse primers after denaturation and annealing; two descendant chains generate from the surface of nanoparticles through the action of DNA polymerase; then, tens of thousands of descendant chains are produced on nanoparticles following multiple rounds of amplification (Fig. 1c). In the decoding process, double fluorescent-labeled probes hybridize with the amplicon from particle phase amplification on the surface of nanoparticles. We employ the auto-signal of nanoparticles and HEV type-specific hybridization signal to translate the encoded barcode. HEV-ID is identified by two fluorescence signals: one identifying nanoparticles, and the other recognizing the hybridization signal on the surface of nanoparticles (Fig. 1d). The unique paired relationship between hybridization probes, the products of particle phase amplification, and nanoparticles, guarantees the accuracy and precision of HEV genotyping detection.

Validation of reproducibility of SSNB

We assessed the reproducibility of this platform by performing SSNB for ten HEV RNA samples in three different batches. Heat map showing the results of the strongest fluorescence signals stand for indicating correct correspondence between HEV and primer-coded nanoparticles and three biological replicates (Fig. 2a–c), demonstrating the high reproducibility and repeatability of the SSNB.

Sensitivity of SSNB in detecting 10 HEV

The sensitivity of the 10-plex SSNB was determined and compared to that of the traditional MHG 10-plex method. The primers and probes used in the MHG and SSNB methods were share the same sequence albeit with different modifications (Supplementary Tables S1 and S2). HEV RNA was analyzed by SSNB and MHG for detecting a ten-fold serially diluted template, separately. The results indicated that the lower limits of detection for SSNB was higher than that of the MHG. Specifically, the sensitivity of SSNB was 10 times higher than that of MHG for CVA10 detection (Fig. 3b), and 1000 times higher than that of MHG for EV71 (Fig. 3d). However, for CVA6, CVA16, CVB1, CVB3, CVB5, E25, E30 and EV-D68, the first gradient template was no detectable using the MHG method (Fig. 3a, c, e–j); thus, we speculate that the sensitivity of SSNB was at least 100 times higher than MHG for CVA6, CVA16, CVB1, at least 10^4 times higher than MHG for CVB5, at least 10^5 times higher than MHG for CVB3, E25, E30, and at least 10^6 times higher than MHG for EV-D68.

In order to further compare the sensitivity of the MHG and SSNB methods, as previously described for the MHG method[18], primers targeting seven viruses including HEV were synthesized (Supplementary Table S3) and used to establish a 7-plex MHG detection method (Supplementary Fig. S1). Subsequently, the aforementioned ten HEV RNA samples were subjected to detection. The sensitivity of SSNB was 10 times higher than that of MHG for CVA6, CVA10 and CVB1 detection (Supplementary Fig. S2a, b, e); 100 times higher than that of MHG for CVB3 and CVB5 (Supplementary Fig. S2f, g); and 1000 times higher than that of MHG for EV71 and E25 (Supplementary Fig. S2d, h). However, for CVA16, E30 and EV-D68, the first gradient template was no detectable using the MHG method (Supplementary Fig. S2c, i, j); thus, we speculate that the sensitivity of SSNB was at least 100 times higher than MHG for CVA16, at least 10^5 times higher than MHG for E30, and at least 10^6 times higher than MHG for EV-D68. The decreased sensitivity observed in the 10-plex MHG compared to the 7-plex MHG can be attributed to the increase in primer sets from seven to ten within the multiplex liquid-phase PCR. This variation may result in more frequent formation of primer dimers or nonspecific amplification products between primers or between primers and templates in traditional MHG method (Supplementary Fig. S3).

10 HEV standards were constructed to verify the detection limit of the 10-plex SSNB method. The findings indicated that the detection limits for CVA6, CVA10, CVA16, EV71, CVB1, CVB3, CVB5, E25, E30, and EV-D68 were 8.10×10^0, 1.25×10^1, 8.10×10^1, 8.10×10^0, 3.94×10^0, 4.30×10^1, 1.14×10^1, 2.70×10^1, 1.27×10^1, and 2.68×10^1 copies/μL, respectively (Supplementary Fig. S4).

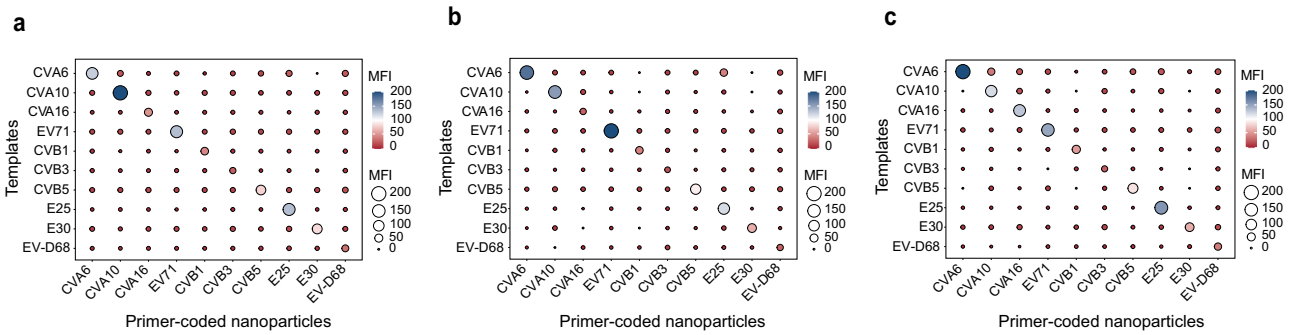

Fig. 2 | Validation of reproducibility and repeatability of SSNB for ten HEV types. a–c Experiments were repeated three independent times at different time points for CVA6, CVA10, CVA16, EV71, CVB1, CVB3, CVB5, E25, E30, EV-D68 detection. Source data are provided as a Source Date file.

https://doi.org/10.1038/s41467-024-50921-w

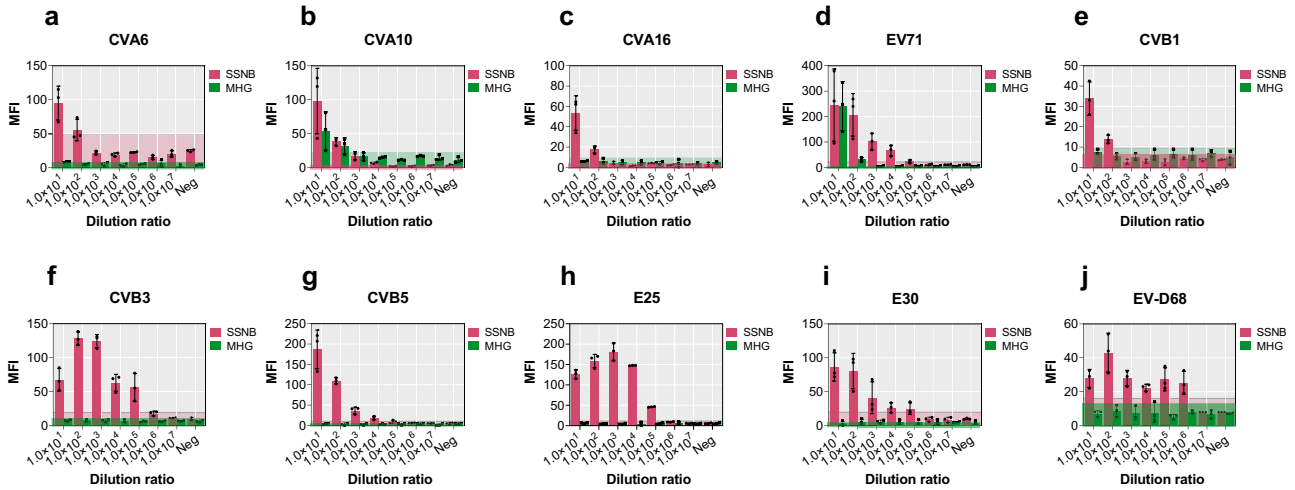

Fig. 3 | The sensitivity of SSNB and MHG detection. a–j The sensitivity comparison results when detected 10 HEV types used SSNB and MHG method. Red shading represents cut-off of SSNB. Green shading represents cut-off of MHG. All experiments were repeated 3 times. "Neg" stands for negative. Error bars represent the means ± standard deviation (S.D.) from replicates. Source data are provided as a Source Date file.

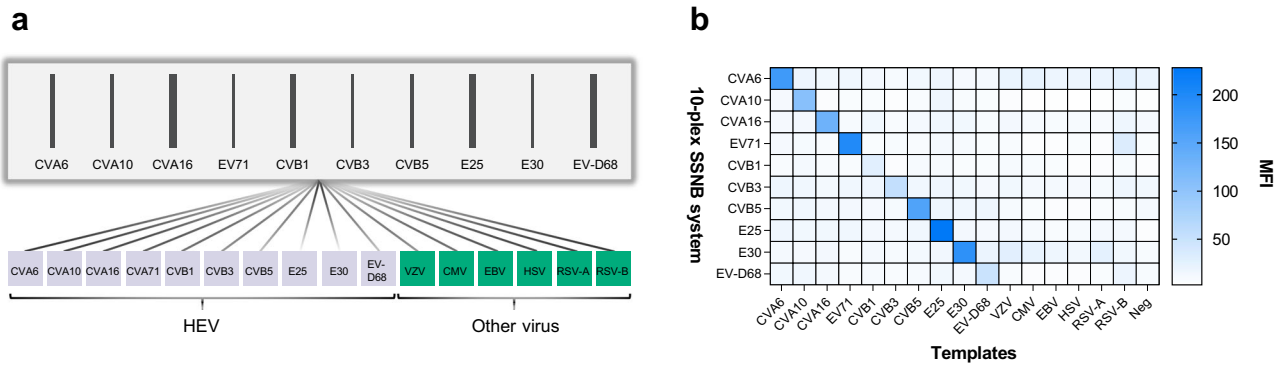

Fig. 4 | Validation of specificity of SSNB. a The reaction was performed with a 10-plex SSNB barcode using 10 different serotypes of HEV and 6 other viruses, respectively. **b** The correspondence between template and primer-coded nanoparticles was displayed in a heatmap using median reporter fluorescence intensity (MFI). VZA Varicella-zoster virus, HCMV human cytomegalovirus, EBV Epstein-Barr virus, HSV herpes simplex virus, RSV-A Respiratory syncytial virus A, RSV-B Respiratory syncytial virus B, Neg negative control. Source data are provided as a Source Date file.

Validation of SSNB specificity

For verification of the specificity of this platform, we performed 10-plex SSNB assays with 10 different serotypes of HEV and 6 other viruses that cause similar clinical symptoms as enteroviruses (Fig. 4a). The results showed that the positive fluorescence signal of 10 HEV types corresponded to their respective specific primer-coded nanoparticles. There was no crosstalk between the 10 types of HEV, or the other 6 viruses, when detection was performed using the 10-plex SSNB system (Fig. 4b). These results suggest a superior detection specificity of SSNB.

Cross infection identification by SSNB

To further evaluate the ability of SSNB to discriminate HEV co-infection, the most common HEV types in clinical settings were selected for pairwise combinations or three combinations to simulate the possible infection conditions. Thirteen dual or triple virus combinations were set and detected by SSNB. The results revealed that for either dual or triple virus combinations, the positive fluorescence signals appeared in only the encoded nanoparticles corresponding the given template (Fig. 5a, b), which suggested that SSNB has excellent capability of discrimination for co-infection.

Validation of the SSNB for use with clinical specimens

The final step in demonstrating the clinical relevance of SSNB involved the use of clinical throat swab samples. The assay results of clinical samples were compared between qRT-PCR[19] and the SSNB method (Fig. 6a). qRT-PCR combined with sequencing is necessary to identify the HEV subtype, while the subtype information can be obtained directly by SSNB. A total of 70 clinical throat swab samples were obtained; of these, 35 were positive for HEV infection and 35 were negative for enterovirus infection according to SSNB (Fig. 6b, c). By qRT–PCR testing, enterovirus infection was detected in 34 of 70 patient swab samples, and 36 were tested as negative (Fig. 6d). The positive predictive agreement and negative predictive agreement values of SSNB relative to the qRT–PCR assay were 100% and 97.22% (Supplementary Table S4), respectively.

Among these positive specimens detected by SSNB, 8 samples were typed for CVA6, 22 samples were typed for CVA16, 2 samples were typed for EV71, and 3 samples were typed for CVB3. All of these positive specimens were confirmed by Sanger sequencing, and the results indicated a 100% successful genotyping rate achieved by the SSNB (Supplementary Table S5).

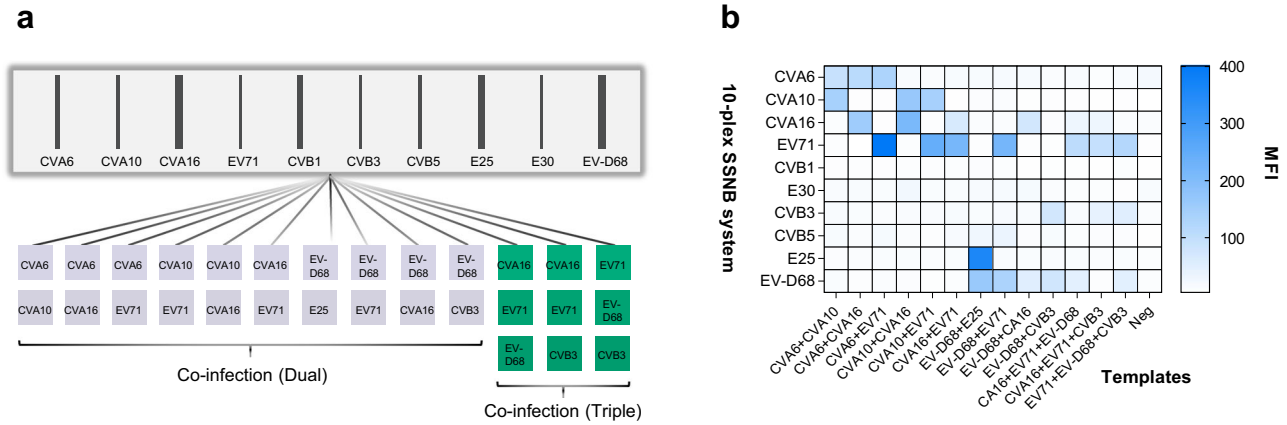

Fig. 5 | Validation of co-infection identification by SSNB. a Two or three HEV types were selected to form a panel and detected by 10-plex SSNB. **b** The results of SSNB are shown as a heatmap using median reporter fluorescence intensity (MFI). Source data are provided as a Source Date file.

Discussion

The natural host for all HEV types is the human[20]: each year, there are over one billion estimated new enterovirus infections. HEV can cause severe neurological and respiratory infections[21], resulting in significant morbidity and mortality as previously seen with EV71 and EV-D68[22–24]. Genotyping detection of HEV is an effective method to prevent against HEV outbreaks and reduce HEV infection-associated diseases.

Existing HEV genotyping strategies typically utilize neutralization assay, RT-PCR, nucleic acid hybridization or sequencing[25–28]. These programs provide accurate validation but have disadvantages, such as the need for complex procedures, inadequate specificity and sensitivity, lack of multiplex detection capability, or need for dedicated bioinformatics facility. In this study, we demonstrate a SSNB platform based on nanoparticle-coded barcode, particle phase surface amplification, and amplicon-mediated dual-labeled probe decoding that offers efficient multiplex HEV genotyping detection capability, high sensitivity and accurate genotyping.

The key challenge in developing a high-multiplex amplification platform is preventing excessive off-target priming by the many primers in the reaction. This study uses surface immobilization of primer pairs to separate reactions and thereby limit primer-dimer formation; as a result, the enhanced multiple detection capability of the SSNB platform does not affect its specificity and sensitivity. This platform has high detection performance: 10 different HEV can be detected via a single sample and reaction, compared with a single sample and reaction detect 1 HEV mode, which improves the convenience of the operation and offers high cost-effectiveness.

In contrast to RT-PCR-based typing methods, the SSNB method offers several advantages, including enhanced detection multiplicity and more efficient utilization of templates. Currently, RT-PCR-based HEV typing methods primarily consist of multiplex RT-PCR and RT-PCR combined with Sanger sequencing. HEV genotyping detection based on multiplex RT-PCR in one-tube typically achieves only 3-4 plex without compromising analytical sensitivity and specificity[13,29]. Developing a method that achieves greater HEV detection multiplicity similar to that of SSNB presents significant challenges due to constraints related to primer dimer formation and limitations of fluorescence channels. Some RT-PCR based methods also require individual single-tube detections for various HEV types, potentially increasing the risk of false negative HEV infection due to inaccurate template distribution across tubes when target concentrations are low. In contrast, the SSNB method enables simultaneous detection of all targets within a single tube, thereby eliminating the risk of missed detections. Furthermore, the RT-PCR and Sanger sequencing hybrid method introduces complexity and extends the detection period[30,31]. When testing clinical samples by RT-PCR and SSNB, the PPA and NPA of SSNB were 100% and 97.22%, respectively. However, one clinical sample was detected as positive by SSNB but negative by RT-PCR negative, which illustrated that SSNB may be superior to or comparable to RT-PCR in terms of clinical specimen detection sensitivity.

Although the MHG method[18] surpasses single-tube multiplex RT-PCR in achieving greater detection multiplicity, covering up to seven virus including HEV, it exhibits lower sensitivity and specificity compared to the SSNB method. Different from SSNB platform that uses surface immobilization primer for particle phase surface amplification, MHG involves multiplex liquid phase amplification before multiplex hybrid reaction. Primer-dimers generated during multiplex liquid phase amplification have a strong influence on the sensitivity, causing the sensitivity of MHG to be fundamentally lower than that of SSNB. Furthermore, when compared with MHG, alongside the sequence-specific DNA-templated reactions, sequence-specific reactions between amplicon and dual-labeled probe are also included, thus giving SSNB excellent specificity performance.

Relative to next generation sequencing (NGS) techniques, the SSNB technique offers a more cost-effective, quicker turnaround time (less than 5 h), without the requirement for specialized bioinformatics analyses, and is easily generalizable because of the universality of clinical detection instruments than sequencers. While NGS holds an advantage in uncovering novel HEV types and remains a gold standard for HEV identification and typing[16]. The SSNB method can effectively complement NGS practices and be adeptly applied across diverse clinical contexts for HEV detection (Supplementary Table S6). For the 35 HEV positive clinical specimens (include 4 types), there was 100% concordance between the gold standard sequencing and SSNB.

It is essential to recognize the limitations of the SSNB typing method, such as the need for multiple liquid transfers and manual processes. Future improvements aimed at refining the SSNB method, along with developing fully automated testing procedures, are expected to mitigate these concerns, making the SSNB method more suited to routine clinical practice.

Together, our results indicate that the SSNB HEV genotyping detection method has good potential for clinical application. We hope to extend SSNB to numerous other HEV genotyping detection platforms in the future, providing evidential basis for rapid and accurate HEV diagnosis, appropriate treatment, and epidemiological investigation.

Methods

Primer and probe design

Given the widespread use of the poliovirus vaccine, the incidence of polio has markedly decreased. However, certain HEVs capable of

https://doi.org/10.1038/s41467-024-50921-w

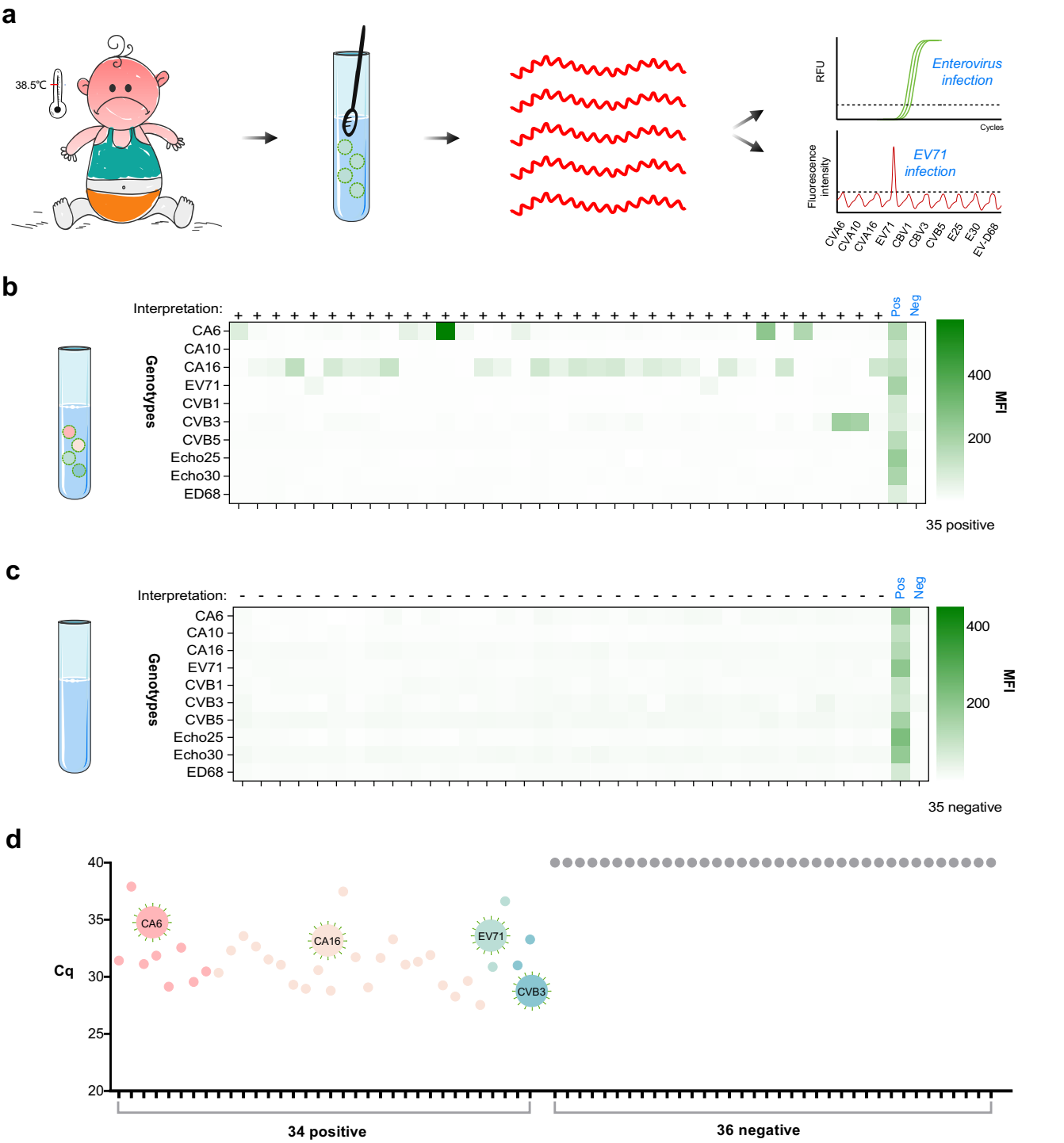

Fig. 6 | SSNB validation in clinical specimens. a A total of 70 clinical samples, highly suspicious for enterovirus infections, were evaluated using the SSNB platform and qRT–PCR assay. **b**, **c** Among the samples, 35 were detected by SSNB as positive for enterovirus and 35 were negative. **d** Among the samples, 34 were detected by qRT-PCR to be positive for enterovirus and 36 negative. Source data are provided as a Source Date file.

causing severe illnesses, including CA6, CA10, CA16, and EV71, which are linked to serious HFMD cases, still lack vaccines. The alternating pattern of infection and seasonal outbreaks typical of HEVs necessitates enhanced surveillance. Considering the epidemiological characteristics, pathogenicity, and surveillance requirements of HEVs, we conducted a careful selection of 10 HEV types for the development of the SSNB system. All nucleotide sequences were obtained from the National Center for Biotechnology Information (NCBI) nucleotide sequence database (GenBank). The *VP1* region of coxsackievirus A6 (CVA6), coxsackievirus A10 (CVA10), coxsackievirus s A16 (CVA16), enterovirus 71 (EV71), coxsackievirus B1 (CVB1), coxsackievirus B3 (CVB3), coxsackievirus B5 (CVB5), echovirus E25 (E25), echovirus E30 (E30), and enterovirus D68 (EV-D68) were aligned using ClustalW (http://www.ebi.ac.uk/clustalw/) in order to identify conserved sequences and specific regions for primer design. Nucleotide-BLAST from NCBI was used to test for homology within the database. All type-specific primer sequences were 5′-amine-C36 modified for subsequent coupling to nanoparticles. Oligonucleotide probes were chosen in

polymorphic sequences amplified by primers and the highly specific section for the particular enterovirus type were selected. 5′ and 3′ ends of probes were modified with 6-carboxytetramethylrhodamine (TAMRA) for compatibility with the detector (Luminex Corporation) and to improve detection sensitivity. All primers and probes (Supplementary Table S1) were purchased from Sangon, China.

Coupling primers to nanoparticles

Fluorescent nanoparticles (Luminex Corporation) were coded by primers. The 5′-amine-C36-modified primers of 10 different HEV types were covalently linked to 10 unique fluorescent nanoparticles, according to the manufacturer's instructions. Using the primer coupling process of one type of HEV as an example: In a reaction volume of 25 μL, 0.8 μM primers and 1×10^5 particles/reaction nanoparticles are included. Next, 1.25 μL of fresh 20 mg/mL EDC is added and the mixture is thoroughly mixed and incubated in darkness for 30 min. The EDC activation coupling step is then repeated. Subsequently, 0.5 mL of 0.02 % Tween-20 is introduced, mixed thoroughly, and the solution is centrifuged at ≥8000 × *g* for 2 min to remove the supernatant. This is followed by the addition of 0.5 mL of 0.1% SDS, thorough mixing, and centrifugation at ≥8000 × *g* for 2 min to eliminate the supernatant. After that, 50 μL of TE buffer (pH 8.0) is added, mixed thoroughly, and the solution is centrifuged at ≥8000 × *g* for 2 min to remove the supernatant. Finally, 200 μL of TE buffer (pH 8.0) is added, the solution is thoroughly mixed, and stored at 4 °C protected from light.

Multiple particle phase amplification

External universal primers were used to enrich the target sequences (Supplementary Table S1). PCR was performed in a 25 μL reaction system, which contained 50 mM Tris-HCl (pH 8.5), 2 mM MgSO4, 70 mM CH3COOK, 200 μM dNTPs, 2 U Taq HS DNA polymerase (TaKaRa), 4 U TransScript Reverse Transcriptase (TransGen Biotech), 0.4 μM of universal primers, and 5 μL of template. Thermal cycling consisted of the reverse transcription step at 50 °C for 10 min, an enzyme activation step at 95 °C for 5 min, followed by thirty cycles of 95 °C for 15 s, and 55 °C for 45 s. PCR was performed on a T100 thermal cycler (Bio-Rad). The products were ligated into a TA cloning vector and verified by Sanger sequencing.

10-plex SSNB was performed on a T100 apparatus (Bio-Rad) for the purpose of generating PCR amplicons on the surface of nanoparticles. DNA amplification was initiated on the nanoparticle surface with a PCR mix containing 1× PCR buffer (TaKaRa), 200 μM dNTPs, 2.5 U SpeedSTAR® HS DNA Polymerase (TaKaRa), 10 different primer-coded nanoparticles (about 3.125×10^3 particles/reaction for each nanoparticle, and 3.125×10^4 particles/reaction for total nanoparticles), and 5 μl of pre-amplification DNA template. PCR was carried out as follows: reactions were heat-denatured at 95 °C for 5 min followed by sixty cycles of 95 °C for 20 s, 60 °C for 30 s, and 72 °C for 30 s and a final 5 min extension step at 72 °C.

Double TAMRA labeled fluorescent probes (0.04 μM for each probe) were hybridized with PCR amplicons. Hybridization procedures consisted of an initial step of 95 °C for 5 min, followed by 55 °C for 5 min. Then, 125 μL of 1× PCR buffer (TaKaRa) was added to each well and the nanoparticles were analyzed by a detector (Luminex 200). The median reporter fluorescence intensity (MFI) of detected nanoparticles was computed for each bead set in the sample. The cutoff value for a positive result was set as twice the MFI value of the negative control.

Enterovirus virus isolation culture

Virus isolation was undertaken in cell culture using human rhabdomyosarcoma or human laryngeal carcinoma (Hep-2) cells (conserved by the National Institute of Diagnostics and Vaccine Development in Infectious Diseases/NIDVD).

Clinical samples

This study was approved by the Ethics Committee of the National Institute of Diagnostics and Vaccine Development in Infectious Diseases (NIDVD). For suspected HFMD patients who visited the Xiamen Haicang Hospital within 1–4 days after symptom onset, samples were collected with throat swabs, eluted into viral transport medium and stored at −80 °C. All patients provided written informed consent.

RNA extraction

For virus-containing cell culture medium, viral RNA was extracted from 200 μL of cell culture supernatant using a magnetic bead nucleic acid extraction kit (GenMagBio) following the manufacturer's instructions. For clinical specimens, throat swab specimens were vortexed and the cotton stick removed before centrifuging for 15 min at 10,000 × *g*. Viral RNA was extracted from 200 μL of throat swab supernatants using a magnetic bead nucleic acid extraction kit (GenMagBio) according to the manufacturer's instructions. RNA was eluted with 50 μL of DEPC-treated water and the Multiskan Spectrum spectrophotometer (Thermo Fisher Scientific) was used to determine the concentrations and the quality of the RNA. The RNA was stored at −20 °C before use.

Traditional MHG method

In the MHG method, sequences of primers and probes consistent with SSNB were employed to detect 10 types of HEV. The differences are in the labeling groups of the primers and probes (Supplementary Table S2) as well as the amplification and detection modalities. cDNA was produced using reverse specific primers extracted RNA in a 20 μL reaction mixture containing 4 U TransScript Reverse Transcriptase (TransGen Biotech), 1× PCR buffer (TaKaRa), 200 μM dNTPs, and the temperature conditions were optimized as 50 °C for 15 min. Multiplex liquid-phase PCR was performed with the Qiagen multiplex PCR plus kit (Qiagen, Hilden, Germany) in a 50 μL reaction mixture containing 25 μL 2× Multiplex PCR Master Mix, 10 different HEV primers, 5 μL cDNA, and the temperature conditions were 95 °C for 15 min, 45 cycles of 94 °C for 30 s, 57 °C for 90 s, 72 °C 30 s, with a final extension step at 72 °C for 10 min. Biotin-labeled PCR products were hybridized with probe-coupled beads under the hybridization condition at 95 °C for 3 min followed by 53 °C for 60 min. The products were then detected after incubation with 5 μg/mL streptavidin-R-phycoerythrin. The cutoff value for a positive result was set as twice the MFI value of the negative control.

Additionally, biotinylated primers and amine-modified probes reported in previous study was used to verify the detection sensitivity of the traditional MHG method for 10 HEV[18]. The reaction conditions and detection process were consistent with those mentioned above. The multiplex liquid-phase PCR assay involves a combination of seven primer pairs (Supplementary Table S3), one of which can detect all types of HEV.

TaqMan real time RT-PCR reaction

TaqMan real-time RT-PCR reaction was performed by the one step method (25 μL PCR reaction system). Each reaction mixture consisted of 50 mM Tris-HCl (pH 8.5), 2 mM MgSO4, 70 mM CH3COOK, 200 μM dNTPs, 2 U Taq HS DNA polymerase (TaKaRa), 8 U TransScript Reverse Transcriptase (TransGen Biotech), 0.4 μM each of EntV-F/R and EntV-P[19] (Supplementary Table S7), and 5 μL template. The thermal cycling protocol comprised the reverse transcription step at 50 °C for 10 min, an enzyme activation step at 95 °C for 5 min, followed by 40 cycles of 95 °C for 15 s and 55 °C for 45 s. PCR was performed on CFX96™ Real-Time System (Bio-Rad).

HEV RNA standards

Plasmids containing the *VP1* gene of HEV along with a T7 promoter sequence were constructed. Single-stranded RNA was generated from the T7 promoter using T7 RNA

polymerase (NEB, USA). Next, plasmid DNA was removed from RNA samples using RNase-free DNase I (Takara, Dalian, China), and the RNA quantified was utilized in subsequent analyses.

Reporting summary

Further information on research design is available in the Nature Portfolio Reporting Summary linked to this article.

Data availability

The data generated in this study are provided in the main text and Supplementary Information. Source data are provided with this paper.

References

1. Wang, K. et al. Serotype specific epitopes identified by neutralizing antibodies underpin immunogenic differences in Enterovirus B. *Nat. Commun.* **11**, 4419 (2020).
2. Sinclair, W. & Omar, M. *Enterovirus* (StatPearls. Press, Treasure Island, 2023).
3. Guo, H. et al. A second open reading frame in human enterovirus determines viral replication in intestinal epithelial cells. *Nat. Commun.* **10**, 4066 (2019).
4. Liu, L. et al. Immunity and clinical efficacy of an inactivated enterovirus 71 vaccine in healthy Chinese children: a report of further observations. *BMC Med.* **13**, 226 (2015).
5. Wu, J. T. et al. Routine Pediatric Enterovirus 71 Vaccination in China: a Cost-Effectiveness Analysis. *PLoS Med.* **13**, e1001975 (2016).
6. Xing, W. et al. Hand, foot, and mouth disease in China, 2008-12: an epidemiological study. *Lancet Infect. Dis.* **14**, 308–318 (2014).
7. Waghmare, A. et al. Clinical disease due to enterovirus D68 in adult hematologic malignancy patients and hematopoietic cell transplant recipients. *Blood* **125**, 1724–1729 (2015).
8. Knoester, M. et al. Upsurge of Enterovirus D68, the Netherlands, 2016. *Emerg. Infect. Dis.* **23**, 140–143 (2017).
9. Dyrdak, R. et al. Outbreak of enterovirus D68 of the new B3 lineage in Stockholm, Sweden, August to September 2016. *Euro Surveill* **21**, https://doi.org/10.2807/1560-7917.ES.2016.21.46.30403 (2016).
10. Melnick, J. L., Schmidt, N. J., Hampil, B. & Ho, H. H. Lyophilized combination pools of enterovirus equine antisera: preparation and test procedures for the identification of field strains of 19 group A coxsackievirus serotypes. *Intervirology* **8**, 172–181 (1977).
11. Huang, K. et al. Antigenic characteristics and genomic analysis of novel EV-A90 enteroviruses isolated in Xinjiang, China. *Sci. Rep.* **8**, 10247 (2018).
12. Xiao, X. L. et al. Simultaneous detection of human enterovirus 71 and coxsackievirus A16 in clinical specimens by multiplex real-time PCR with an internal amplification control. *Arch. Virol.* **154**, 121–125 (2009).
13. Beuret, C. Simultaneous detection of enteric viruses by multiplex real-time RT-PCR. *J. Virol. Methods* **115**, 1–8 (2004).
14. Kandolf, R., Ameis, D., Kirschner, P., Canu, A. & Hofschneider, P. H. In situ detection of enteroviral genomes in myocardial cells by nucleic acid hybridization: an approach to the diagnosis of viral heart disease. *Proc. Natl Acad. Sci. USA* **84**, 6272–6276 (1987).
15. Rotbart, H. A. Nucleic acid detection systems for enteroviruses. *Clin. Microbiol. Rev.* **4**, 156–168 (1991).
16. Harvala, H. et al. Recommendations for enterovirus diagnostics and characterisation within and beyond Europe. *J. Clin. Virol.* **101**, 11–17 (2018).
17. Anderson, G. P., Kowtha, V. A. & Taitt, C. R. Detection of fumonisin b1 and ochratoxin a in grain products using microsphere-based fluid array immunoassays. *Toxins* **2**, 297–309 (2010).
18. Hamza, I. A., Jurzik, L. & Wilhelm, M. Development of a Luminex assay for the simultaneous detection of human enteric viruses in sewage and river water. *J. Virol. Methods* **204**, 65–72 (2014).
19. Monpoeho, S. et al. Quantification of enterovirus RNA in sludge samples using single tube real-time RT-PCR. *Biotechniques* **29**, 88–93 (2000).
20. Kotani, O. et al. Neuropathogenicity of Two Saffold Virus Type 3 Isolates in Mouse Models. *PLoS One* **11**, e0148184 (2016).
21. Good, C., Wells, A. I. & Coyne, C. B. Type III interferon signaling restricts enterovirus 71 infection of goblet cells. *Sci. Adv.* **5**, eaau4255 (2019).
22. Solomon, T. et al. Virology, epidemiology, pathogenesis, and control of enterovirus 71. *Lancet Infect. Dis.* **10**, 778–790 (2010).
23. Schuffenecker, I. et al. Epidemiological and clinical characteristics of patients infected with enterovirus D68, France, July to December 2014. *Euro Surveill.* **21**, https://doi.org/10.2807/1560-7917.ES.2016.21.19.30226 (2016).
24. Casas-Alba, D. et al. Outbreak of brainstem encephalitis associated with enterovirus-A71 in Catalonia, Spain (2016): a clinical observational study in a children's reference centre in Catalonia. *Clin. Microbiol. Infect.* **23**, 874–881 (2017).
25. Saarinen, N. V. V. et al. Multiplexed High-Throughput Serological Assay for Human Enteroviruses. *Microorganisms* **8**, https://doi.org/10.3390/microorganisms8060963 (2020).
26. Gregory, J. B., Litaker, R. W. & Noble, R. T. Rapid one-step quantitative reverse transcriptase PCR assay with competitive internal positive control for detection of enteroviruses in environmental samples. *Appl. Environ. Microbiol.* **72**, 3960–3967 (2006).
27. Chapman, N. M., Tracy, S., Gauntt, C. J. & Fortmueller, U. Molecular detection and identification of enteroviruses using enzymatic amplification and nucleic acid hybridization. *J. Clin. Microbiol.* **28**, 843–850 (1990).
28. Joffret, M. L. et al. Whole Genome Sequencing of Enteroviruses Species A to D by High-Throughput Sequencing: Application for Viral Mixtures. *Front. Microbiol.* **9**, 2339 (2018).
29. Zhang, S. et al. A one-step, triplex, real-time RT-PCR assay for the simultaneous detection of enterovirus 71, coxsackie A16 and pan-enterovirus in a single tube. *PLoS One* **9**, e102724 (2014).
30. Oberste, M. S. et al. Typing of human enteroviruses by partial sequencing of VP1. *J. Clin. Microbiol.* **37**, 1288–1293 (1999).
31. Gulholm, T. et al. Molecular typing of enteroviruses: comparing 5′UTR, VP1 and whole genome sequencing methods. *Pathology* **54**, 779–783 (2022).

Acknowledgements

This work was supported by the National Natural Science Foundation of China (81991491), Science and Technology Key Project in Fujian Province (2020YZ015004), Fujian Provincial Health Commission for Medical Research Program (2021ZD01006), the CAMS Innovation Fund for Medical Sciences (2019RU022), and the Fundamental Research Funds for the Central Universities (20720220006).

Author contributions

Z.C.Z., X.S.S., K.Y.Y., S.X.G., S.Y.Z. and N.S.X. conceived the project. Z.C.Z., X.S.S., K.Y.Y., W.D.H., J.W., Z.H.Z., J.Y.X. and L.S.L. performed the experiments. S.Z.H. and T.D.L helped to prepare the figures. J.Z. provided suggestions for manuscript editing. Z.C.Z., X.S.S. and K.Y.Y. analyzed the data and co-wrote the manuscript. S.X.G., S.Y.Z. and N.S.X. approved the final version of the manuscript. All authors contributed to discussions.

Competing interests

The authors declare no competing interests.

Additional information

Supplementary information The online version contains supplementary material available at https://doi.org/10.1038/s41467-024-50921-w.

Correspondence and requests for materials should be addressed to Shengxiang Ge, Shiyin Zhang or Ningshao Xia.

Peer review information *Nature Communications* thanks Chien-Fu Chen, and the other, anonymous, reviewer for their contribution to the peer review of this work. A peer review file is available.

Reprints and permissions information is available at http://www.nature.com/reprints

Publisher's note Springer Nature remains neutral with regard to jurisdictional claims in published maps and institutional affiliations.

Open Access This article is licensed under a Creative Commons Attribution-NonCommercial-NoDerivatives 4.0 International License, which permits any non-commercial use, sharing, distribution and reproduction in any medium or format, as long as you give appropriate credit to the original author(s) and the source, provide a link to the Creative Commons licence, and indicate if you modified the licensed material. You do not have permission under this licence to share adapted material derived from this article or parts of it. The images or other third party material in this article are included in the article's Creative Commons licence, unless indicated otherwise in a credit line to the material. If material is not included in the article's Creative Commons licence and your intended use is not permitted by statutory regulation or exceeds the permitted use, you will need to obtain permission directly from the copyright holder. To view a copy of this licence, visit http://creativecommons.org/licenses/by-nc-nd/4.0/.

© The Author(s) 2024